

Electronic Supporting Information

Synthesis and photophysical characterization of porphyrin and porphyrin-Ru(II) polypyridyl chromophore–catalyst assemblies on mesoporous metal oxides†

Animesh Nayak,[‡] Robin R. Knauf,[‡] Kenneth Hanson, Leila Alibabaei, Javier J. Concepcion, Dennis L. Ashford, Jillian L. Dempsey* and Thomas J. Meyer*

*Department of Chemistry, The University of North Carolina at Chapel Hill, Chapel Hill, North Carolina 27599, USA. E-mail:
dempseyj@email.unc.edu, tjmeyer@unc.edu*

Experimental:

Materials All reagents and solvents were obtained from either Sigma Aldrich or Fisher Scientific and used without any purification. Inert atmosphere manipulations were carried out under argon prepurified by passage through a drying tower (Linde 3-Å molecular sieves). Deuterated solvents CDCl₃ and CD₃OD for NMR were obtained from Cambridge Isotope Laboratories Inc. Nano-TiO₂, ZrO₂ and SnO₂ films on top of FTO (fluorine doped SnO₂) coated glass were prepared according to previously published methods.¹⁻³

Instrumentation:

Transient Absorption Spectroscopy Nanosecond to microsecond transient absorption experiments were performed using a commercially available laser flash photolysis system (Edinburgh Instruments, Inc., model LP920). Laser excitation (425 nm, 5-7 ns FWHM, 3.8 ± 0.1 mJ/pulse, 15mJ/cm² unless stated otherwise) was provided by a pulsed Nd:YAG laser (Spectra-Physics, Inc., model Quanta-Ray LAB-170-10) / OPO (VersaScan-MB) combination. To accommodate the pulsed, 1 Hz intensification of the 450W Xe probe source of the LP920, the laser system was set such that the flashlamps were fired at 10 Hz yet Q-switched at 1 Hz. Timing of the experiment, including laser and probe pulsing, as well as data collection was PC controlled via Edinburgh software (L900) with the aid of a Tektronix oscilloscope (model TDS-3032C). The LP920 white light probe output was passed through a 380 nm long pass color

filter before passing through the sample to minimize band gap excitation of SnO₂. The LP920 was equipped with a multi-grating detection monochromator outfitted with a Hamamatsu R928 photomultiplier tube (PMT) in a non-cooled housing and a gated CCD (Princeton Instruments, PI-MAX3) such that detection was software selectable. The gated CCD was used for recording transient spectra of SnO₂-3 and ZrO₂-3 covering the visible region (400-850 nm, 3 nm spectral bandwidth) at a given time after excitation (10 ns gatewidth). Data were the result of averaging 100-200 laser shots. The transient spectral data for complex SnO₂-1, ZrO₂-1, SnO₂-1-Zr-2 and ZrO₂-1-Zr-2 were generated from kinetic traces measured with the PMT. Kinetics were taken every 5-10 nm, and were the result of averaging 30-50 laser shots. Spectral data were analyzed using Igor Pro (WaveMetrics Inc.) software. Data were collected at room temperature (295 ± 3 K). Derivatized MO₂ films were inserted diagonally into a 10 mm path length quartz cuvette whose top had been adapted with a #15 o-ring sealing joint, sidearm, and Kontes valve. After addition of solvent (0.1 M LiClO₄ in acetonitrile or aqueous 0.1 M HClO₄) to the cuvette, the sample was sparged with argon for at least 45 minutes immediately prior to experiments.

Steady-State Emission data were collected at room temperature using an Edinburgh FLS920 spectrometer with luminescence first passing through a 450 nm long-pass color filter, then a single grating (1800 l/mm, 500 nm blaze) Czerny-Turner monochromator (10 nm bandwidth) and finally detected by a peltier-cooled Hamamatsu R2658P photomultiplier tube. Samples were excited at 425 nm using light output from a housed 450 W Xe lamp / single grating (1800 l/mm, 250 nm blaze) Czerny-Turner monochromator combination with 10 nm bandwidth and a 375 nm long pass filter to avoid direct excitation of the metal oxide.

Time Resolved Emission dynamics were monitored using the FLS920's time-correlated single-photon counting capability (1024 channels; 1 ns per channel) with each data set collecting a set number of counts. Excitation was provided by an Edinburgh EPL-445 picosecond pulsed diode laser (444.2 nm, 80 ps FWHM) operated at 20 MHz. Derivatized metal oxide samples were placed in a two piece cuvette and Argon degassed as described for the TA measurements.

Spectroelectrochemistry Spectroelectrochemistry was carried out in CH₃CN (0.1 M [Bu₄N][PF₆]) using a honeycomb cell and Ag/AgCl nonaqueous reference electrode. Ferrocene

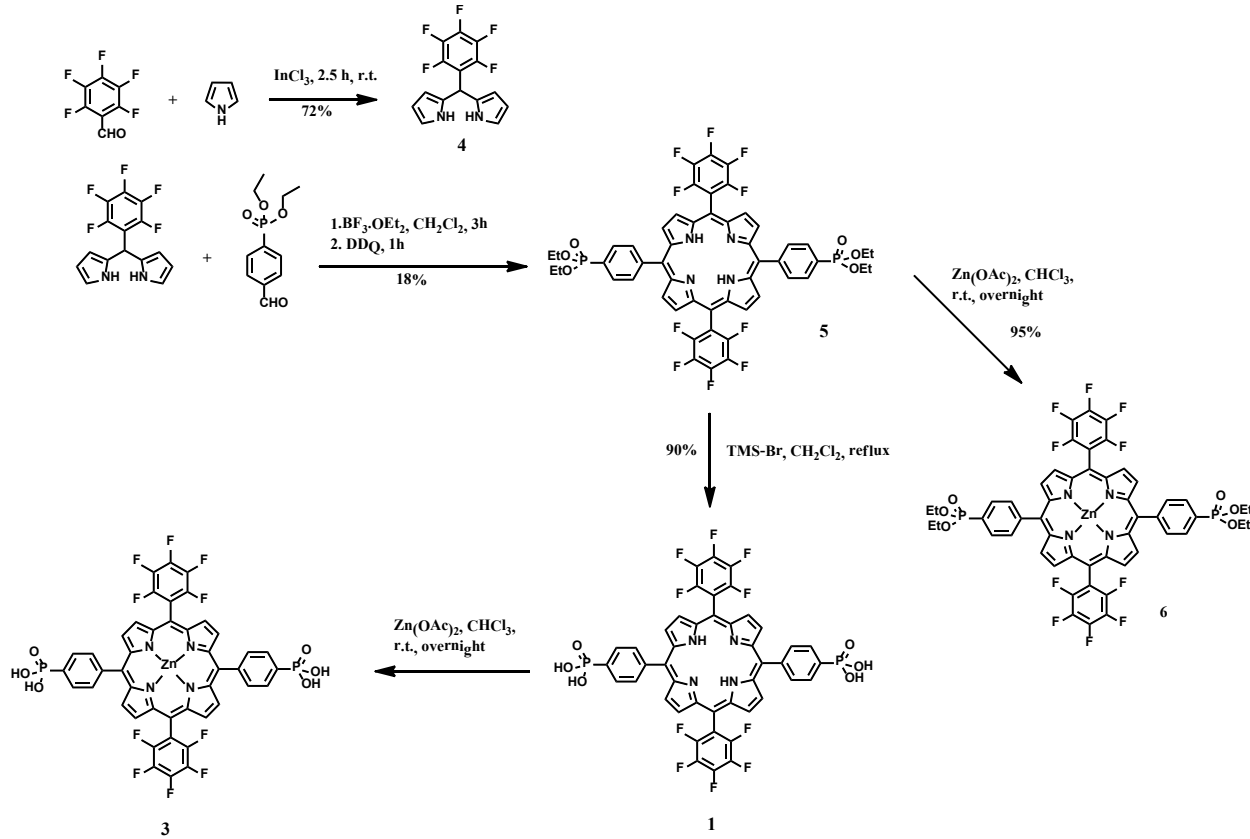
was then used as an internal standard ($E^{\circ'} (\text{Fc}^{+/0}) = + 630\text{mV}$ vs. NHE).⁴ Inert atmosphere was maintained by performing experiments in a nitrogen-filled glovebox. Linear staircase voltammetry was used, with a 2 minute hold time and 100 mV step size. Absorbance spectra were measured at each step. The data are reported as a difference spectra of the absorbance at the specified potential minus the absorbance without a potential applied.

Cyclic Voltammetry Cyclic voltammetry of compounds **5** and **6** in solution was performed in CH_2Cl_2 (0.1 M [$^n\text{Bu}_4\text{N}][\text{PF}_6]$]) using a 3-cell set up with a glassy carbon as working, nonaqueous Ag/AgNO_3 as reference and a Pt wire as counter electrode. Inert atmosphere was maintained by purging argon through the solution for 2 min before scans. Ferrocene was used as an internal standard ($E^{\circ'} (\text{Fc}^{+/0}) = + 690 \text{ mV}$ vs. NHE).

X-ray photoelectron spectroscopy XPS data was taken on a Kratos Axis Ultra DLD system equipped with a monochromatic Al Ka x-ray source. The XPS chamber had a base pressure of ca. 5×10^{-9} torr and a pass energy of 20 eV was used for all high resolution scans.

Synthesis:

5-(Pentafluorophenyl)dipyrromethane⁵ (**4**) and 4-(di-ethoxyphosphoryl)benzaldehyde⁶ was synthesized following literature procedures. Synthesis of **2** was reported previously.⁷



5,15-Bis[4-(diethoxyphosphoryl)phenyl]-10,20-bis(pentafluorophenyl)porphyrin (5) A solution of 5-(Pentafluorophenyl)dipyrromethane (300 mg, 0.96 mmol) and 4-(Di-*tert*-ethoxyphosphoryl)benzaldehyde (233 mg, 0.96 mmol) in methylene chloride (250mL) was degassed by passing Ar through the solution for 15 min. BF₃.OEt₂ (0.05mL) was added and the solution was stirred at r.t. for 3h during which time color of the solution changed to red. After 3h, 2,3-dicloro-5,6-dicyano-1,4-benzoquinone (350 mg, 1.54 mmol) was added and the mixture was stirred for another 1h. The crude mixture was then passed through a silica pad and the purple band was collected. The compound was purified by silica gel column chromatography using 98:2 CH₂Cl₂/MeOH mixture as eluant. The major purple band was collected. Purple crystals of the pure compound were obtained after recrystallization from MeOH; 92mg, 18% yield. ¹H NMR (400 MHz, CDCl₃) δ 8.89 (d, *J* = 4.8 Hz, 4H), 8.82 (d, *J* = 4.8 Hz, 4H), 8.32 (m, 4H), 8.22 (m, 4H), 4.38 (m, 8H), 1.52 (t, *J* = 7.1 Hz, 12H), -2.88 (s, 2H); ¹⁹F NMR (400 MHz, CDCl₃) δ -136.82 (dd, *J* = 26 Hz, *J* = 8Hz, 2F), δ -151.93 (t, *J* = 20 Hz, 1F), δ -161.74 (td, *J* = 25 Hz, *J* = 8Hz, 2F); ³¹P NMR (400 MHz, CDCl₃) δ -18.60; ESI-MS: 1067.20 (Calcd for M+H = 1067.22);

Zinc(II)-5,15-bis[4-(Diethoxyphosphoryl)phenyl]-10,20-bis(pentafluorophenyl)porphyrin (6)

In a solution of **5** (75 mg, 0.07 mmol) in chloroform (200mL) and methanol (2mL) zinc acetate (150 mg, 0.68 mmol) was added. The mixture was then stirred at r.t. for 16h. The solution was then washed with water (3x100 mL) and organic phase was dried over anhyd. Na₂SO₄. After solvent was removed the compound was purified from the crude mixture silica gel column chromatography using 98:2 CH₂Cl₂/MeOH mixture as eluant. The major purple band was collected and solvent was removed to get 75 mg (95% yield based on initial free base porphyrin **5**) of purple solid. ¹H NMR (400 MHz, CD₃OD) δ 8.97 (d, *J* = 4.6 Hz, 4H), 8.89 (d, *J* = 4.6 Hz, 4H), 8.41 (m, 4H), 8.19 (m, 4H), 4.37 (m, 8H), 1.51 (t, *J* = 7.2 Hz, 12H); ¹⁹F NMR (400 MHz, CD₃OD) δ -140.33 (dd, *J* = 25 Hz, *J* = 8Hz, 2F), δ -156.98 (t, *J* = 20 Hz, 1F), δ -166.01 (td, *J* = 25 Hz, *J* = 8Hz, 2F); ³¹P NMR (400 MHz, CD₃OD) δ -19.49; ESI-MS: 1129.13 (Calcd for M+H = 1129.13).

5,15-Bis[4-(dihydroxyphosphoryl)phenyl]-10,20-bis(pentafluorophenyl)porphyrin (1) In a solution of **5** (50 mg, 0.047 mmol) in anhyd. CH₂Cl₂ (8 mL) was added neat trimethylsilyl bromide (62 μL, 0.47 mmol). The mixture was refluxed under Ar for 1 day. After removing solvent, the solid product was suspended in water and stirred for 4h. The solid material was filtered to get the product as a purple solid (40mg, 90% yield based on **5**). ¹H NMR (400 MHz, CD₃OD) δ 9.06 (br s 4H), 8.95 (br s 4H), 8.37 (m, 4H), 8.25 (m, 4H); ¹⁹F NMR (400 MHz, CD₃OD) δ -140.62 (dd, *J* = 25 Hz, *J* = 8Hz, 2F), δ -154.89 (t, *J* = 20 Hz, 1F), δ -164.87 (td, *J* = 25 Hz, *J* = 8Hz, 2F); ³¹P NMR (400 MHz, CD₃OD) δ -15.47.

Zinc(II)-5,15-bis[4-(Dihydroxyphosphoryl)phenyl]-10,20-bis(pentafluorophenyl)porphyrin (3)

(3) In a solution of **1** (20 mg, 0.021 mmol) in CH₂Cl₂/MeOH (5mL/2mL), was added zinc acetate (23 mg, 0.11 mmol) and stirred at r.t. Progress of the reaction was monitored by UV-vis. After 18 h, when the absorption change was complete, the mixture was washed with water, organic phase was collected and concentrated to be used as a stock solution.

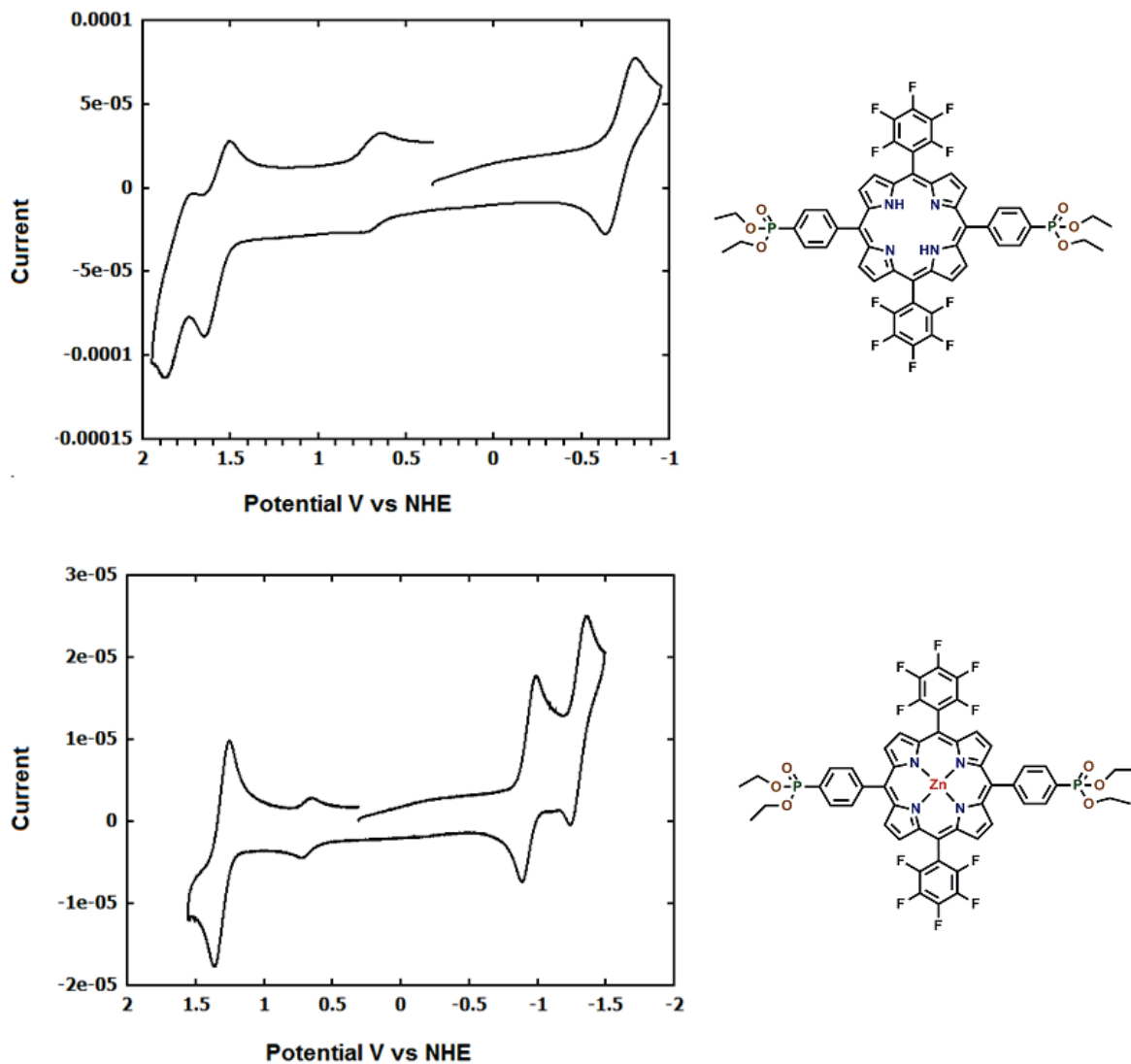


Figure S1: Cyclic voltammetry of free base (**5**) and Zn-porphyrin (**6**) in $0.1 \text{ M} [^n\text{Bu}_4\text{N}] [\text{PF}_6]$ in CH_2Cl_2 . Scan rate = 100 mV/sec. Ferrocene was used as an internal standard ($E^{\circ'} (\text{Fc}^{+/0}) = + 690 \text{ mV}$ vs. NHE).

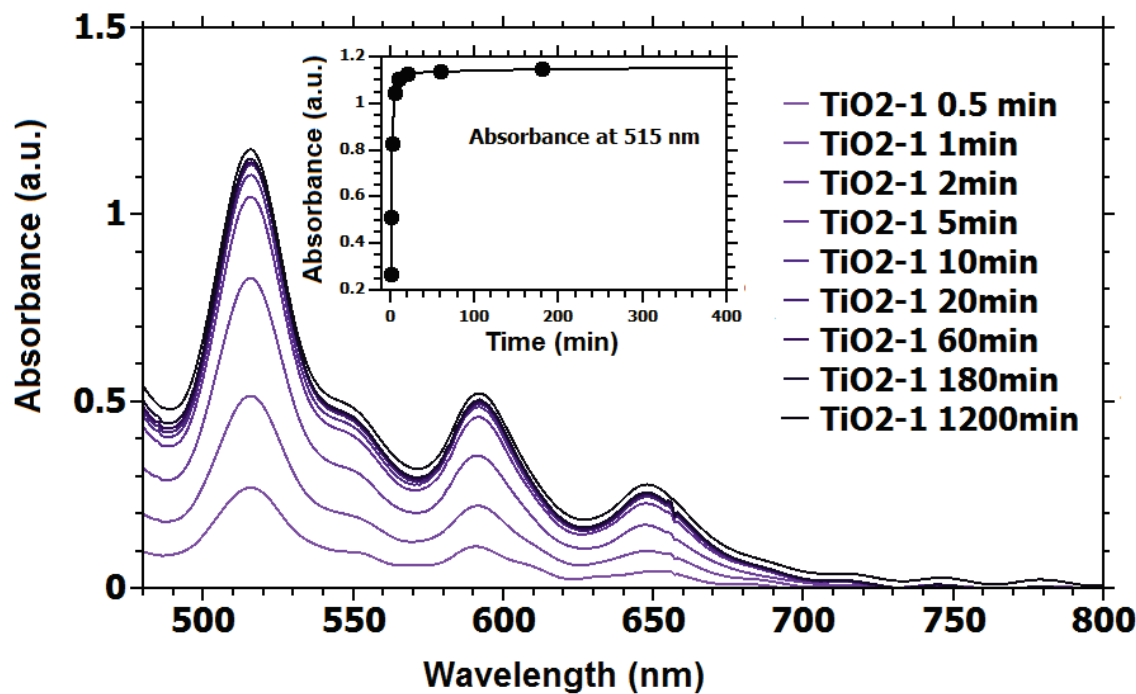


Figure S2: Loading of $\text{TiO}_2\text{-1}$ ($\sim 7\mu\text{m}$ thick nanocrystalline TiO_2 film) from a 1.2 mM solution of **1** in $\text{CH}_2\text{Cl}_2/\text{MeOH}$ (1:1) as a function of time.

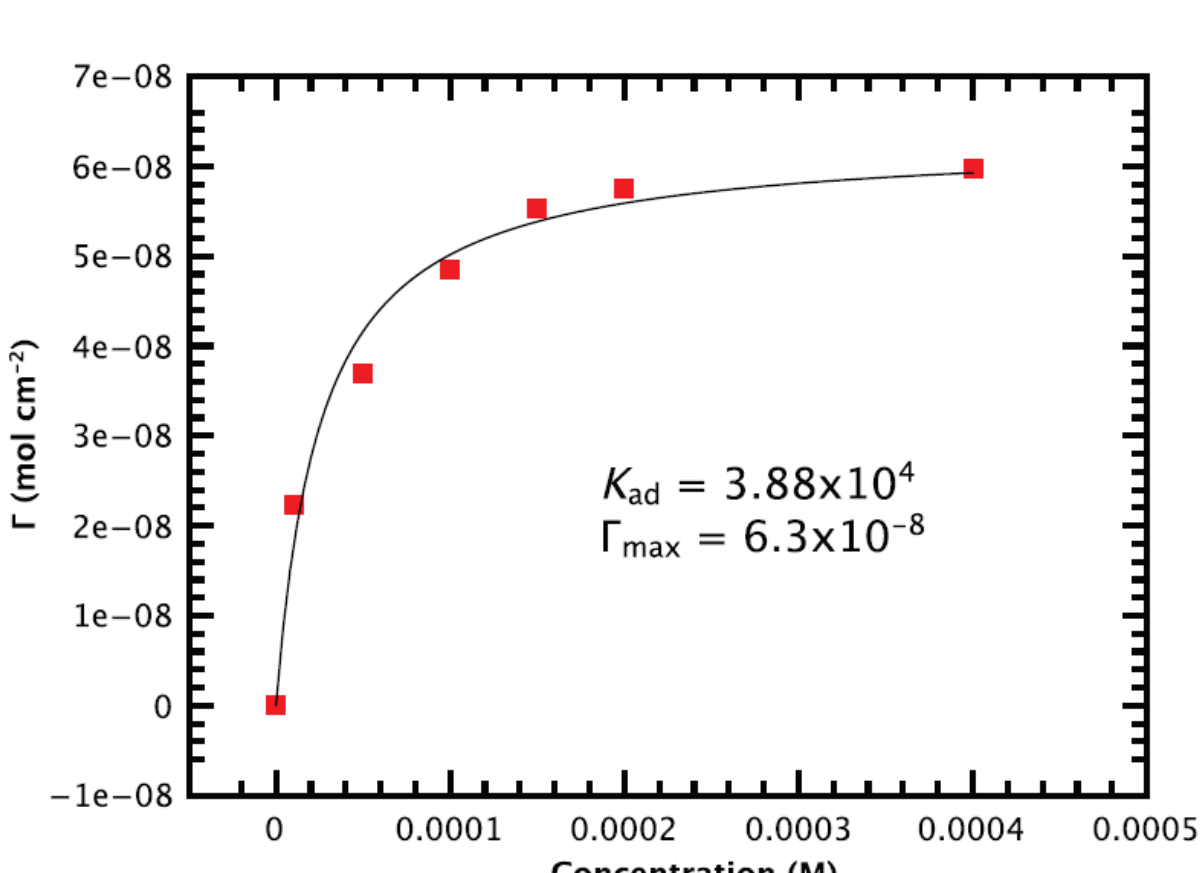


Figure S3: Adsorption isotherm of TiO₂–1 in CH₂Cl₂/MeOH (1:1).

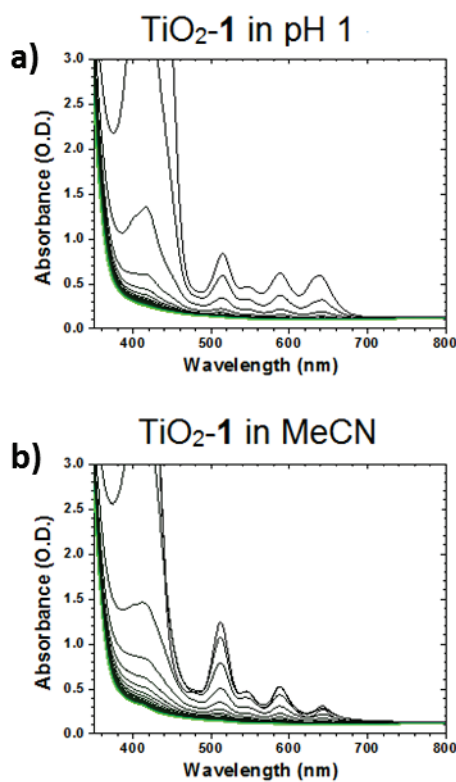
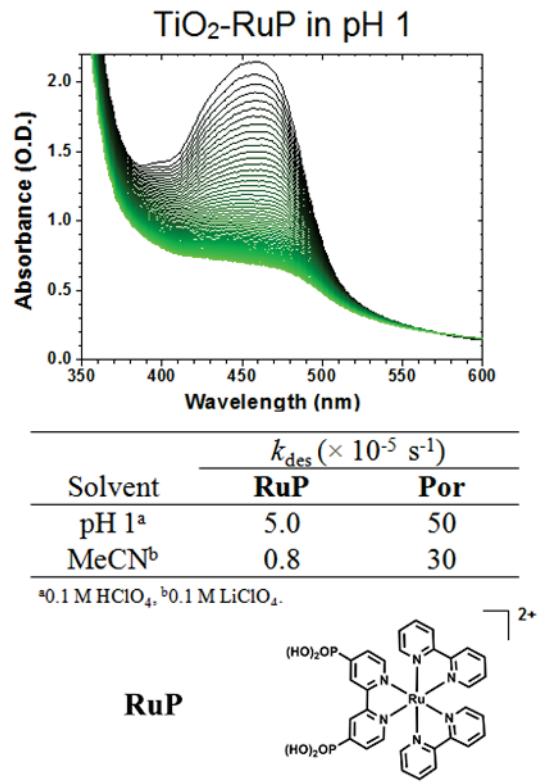


Figure S4: Photostability measurements of TiO₂-1 in a) 0.1 M HClO₄ and b) CH₃CN (0.1 M LiClO₄). Samples were irradiated with a 455 nm LED light, ~30 nm fwhm, 475 mW/cm².

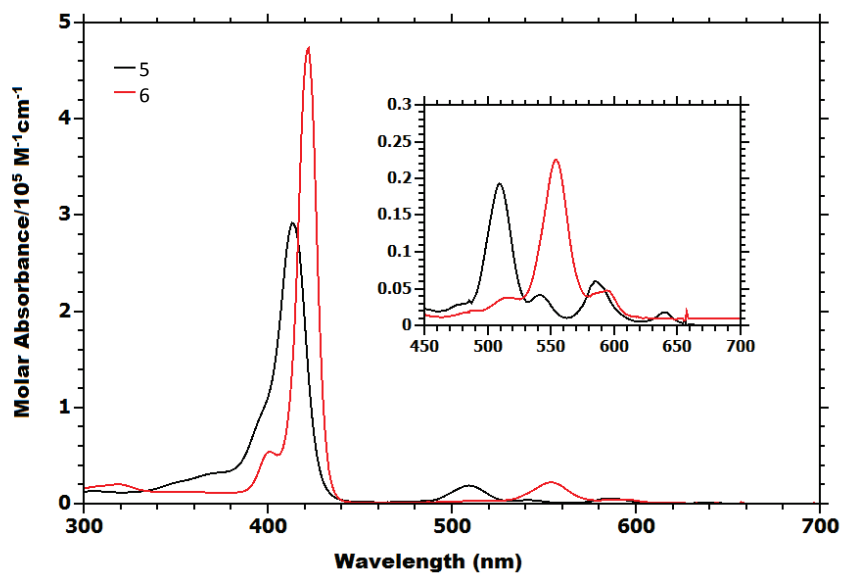


Figure S5: Ground state absorption spectra of **5** (black line) and **6** (red line) in 1:1 $\text{CH}_2\text{Cl}_2/\text{MeOH}$.

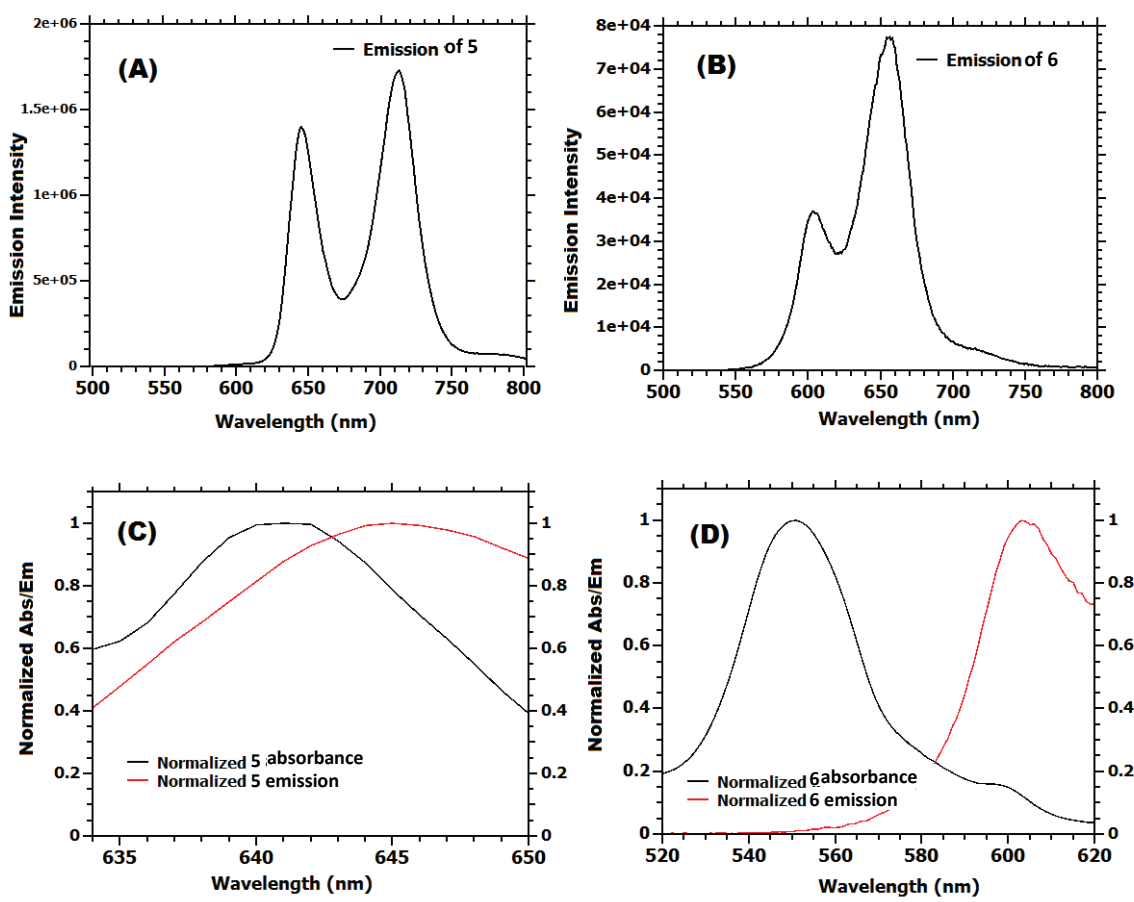


Figure S6: Steady state emission of **5** (A) and **6** (B) in CH_2Cl_2 measured at 25°C . (C) and (D) show cross sections of normalized absorption and emission for **5** and **6** respectively.

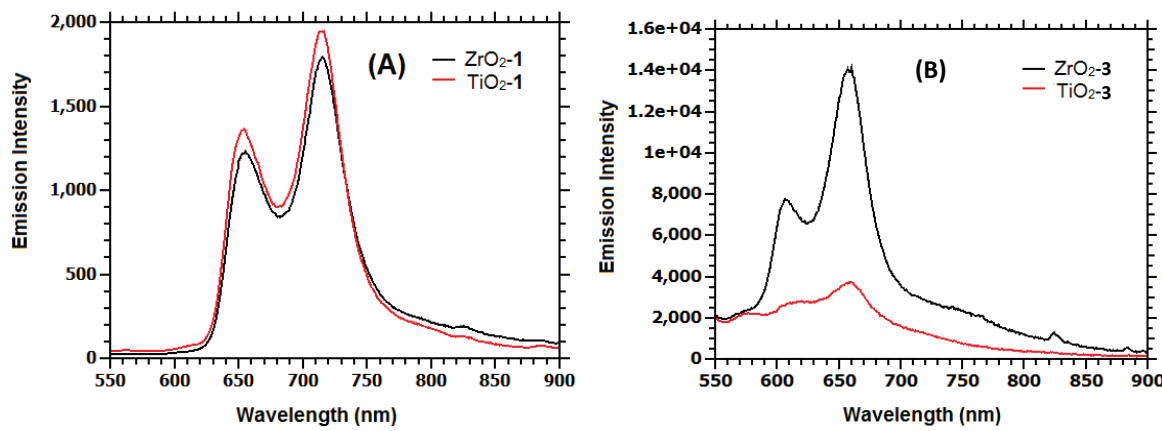


Figure S7: Comparison of emission quenching **1** and **3** loaded on TiO_2 and ZrO_2 in CH_3CN (0.1 M LiClO_4).

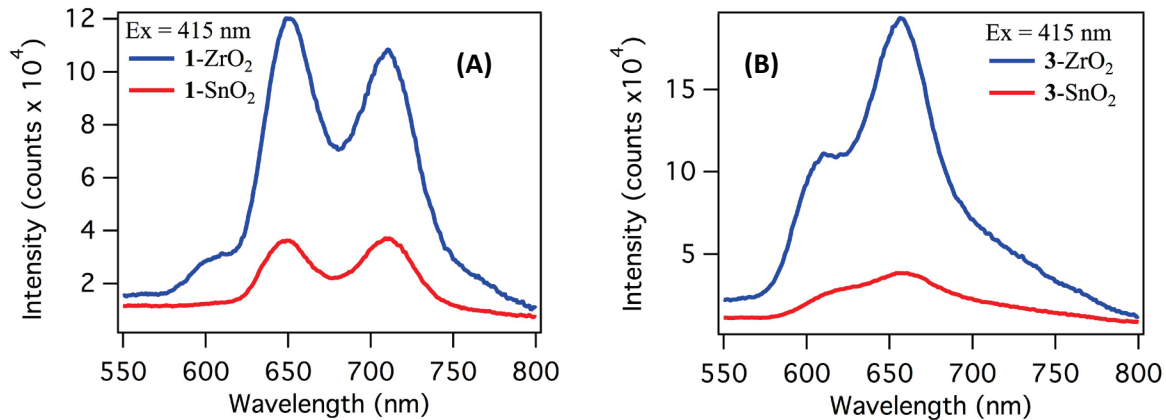


Figure S8: Comparison of emission quenching of **1** and **3** loaded on SnO_2 and ZrO_2 in CH_3CN (0.1 M LiClO_4).

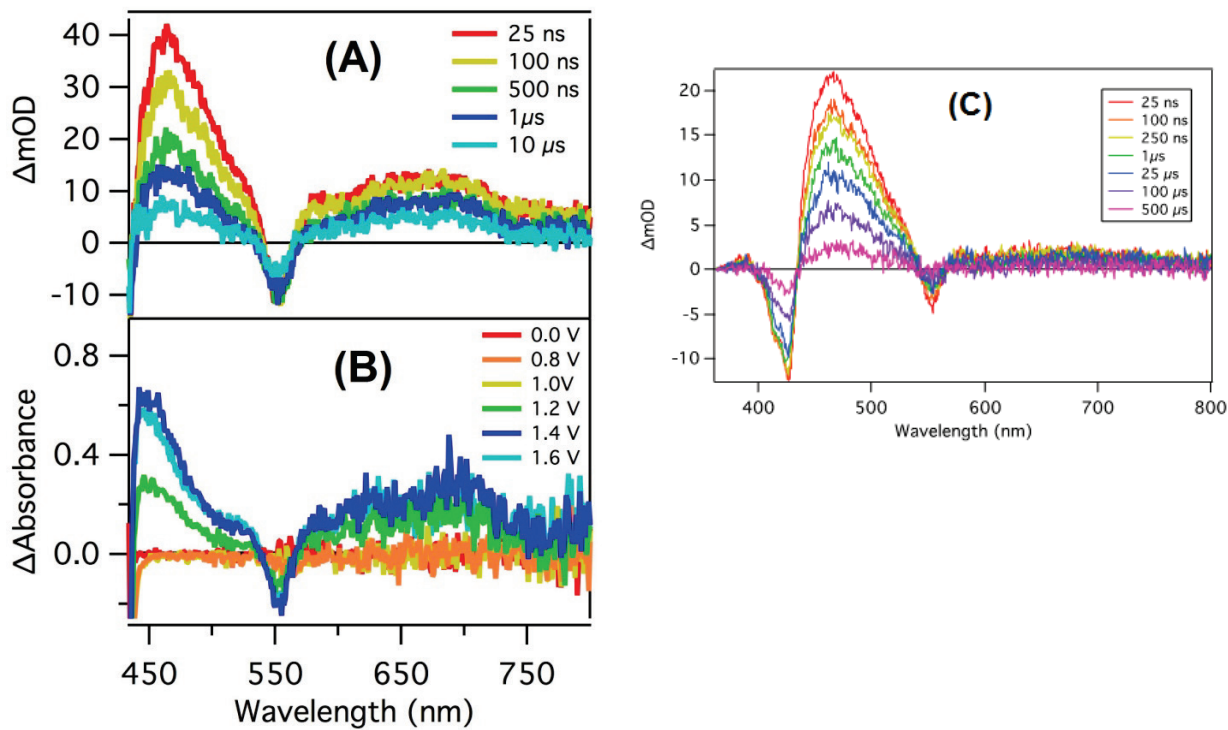


Figure S9: (A) Time dependent transient absorption difference spectra for $\text{SnO}_2\text{-3}$ following 425 nm excitation in CH_3CN (0.1 M LiClO_4) (B) $\text{P}^+ - \text{P}$ absorption difference spectra for $\textbf{6}$ in MeCN (0.1 M $[\text{Bu}_4\text{N}][\text{PF}_6]$) as a function of applied potential as determined via a spectroelectrochemical titration. Potentials referenced vs. Ag/AgCl . (C) Time dependent transient absorption difference spectra for $\text{ZrO}_2\text{-3}$ in CH_3CN (0.1 M LiClO_4) after excitation at 425 nm.

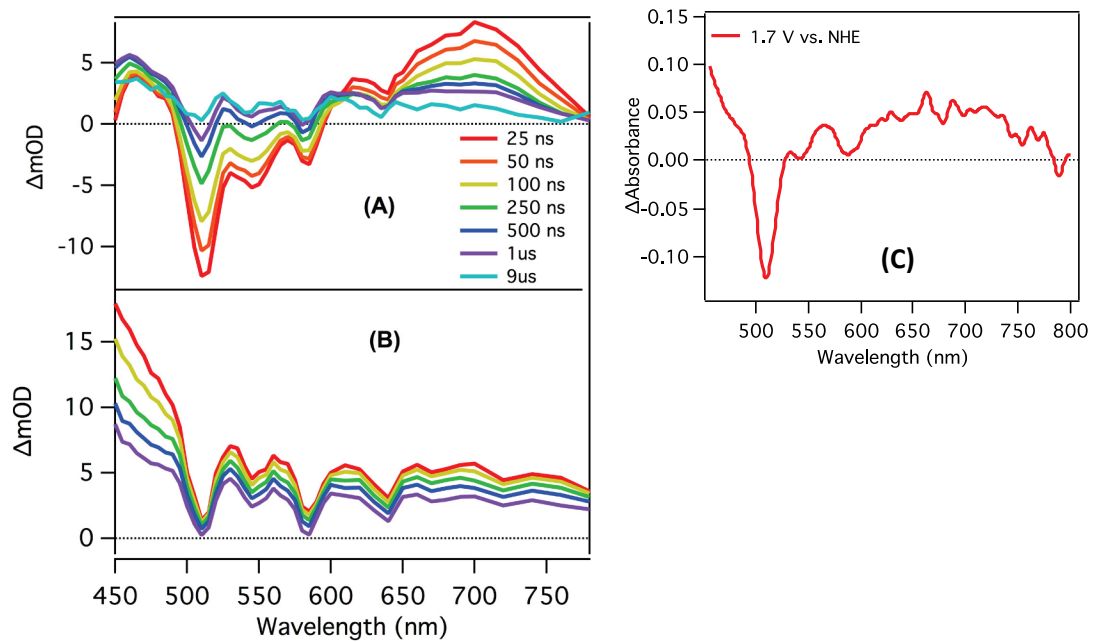


Figure S10: (A) Time dependent transient absorption difference spectra for $\text{SnO}_2\text{-1}$ following 425 nm excitation in CH_3CN (0.1 M LiClO_4) (B) Time dependent transient absorption difference spectra for $\text{ZrO}_2\text{-1}$ following 425 nm excitation in CH_3CN (0.1 M LiClO_4) . (C) $\text{P}^+\text{-P}$ absorption difference spectra for **5** in MeCN (0.1 M $[\text{Bu}_4\text{N}] [\text{PF}_6]$) at 1.7 V vs. NHE as determined via a spectroelectrochemical titration.

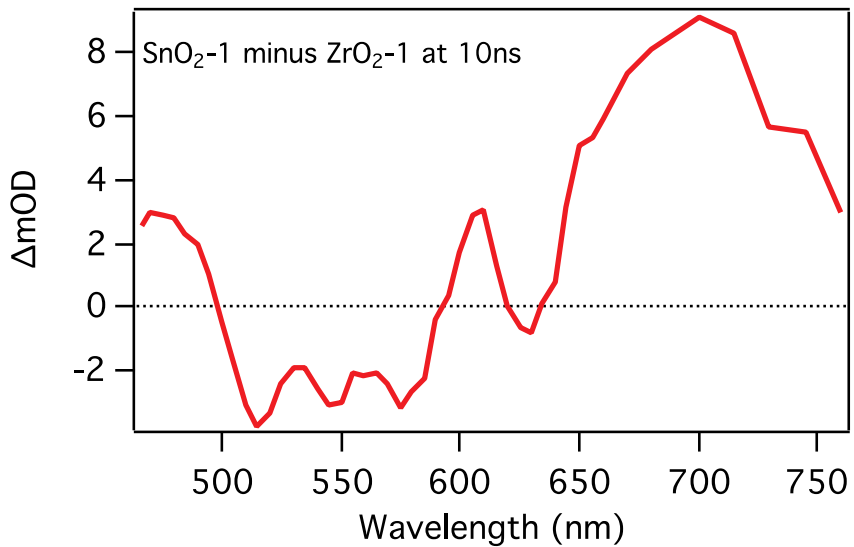


Figure S11: Subtraction of $\text{ZrO}_2\text{-1}$ TA spectrum at 10 ns (scaled) from $\text{SnO}_2\text{-1}$ TA spectrum at 10 ns, illustrating the formation of 1^+ in aqueous 0.1 M HClO_4 .

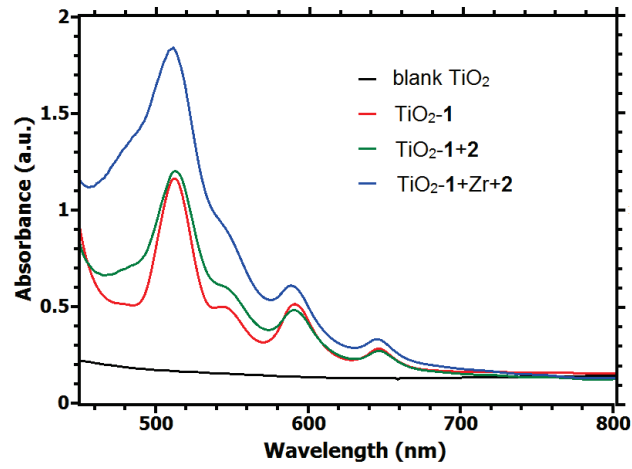


Figure S12: Absorption spectrum of the 1:1 chromophore-catalyst assembly $\text{TiO}_2\text{-1-Zr-2}$ in CH_3CN .

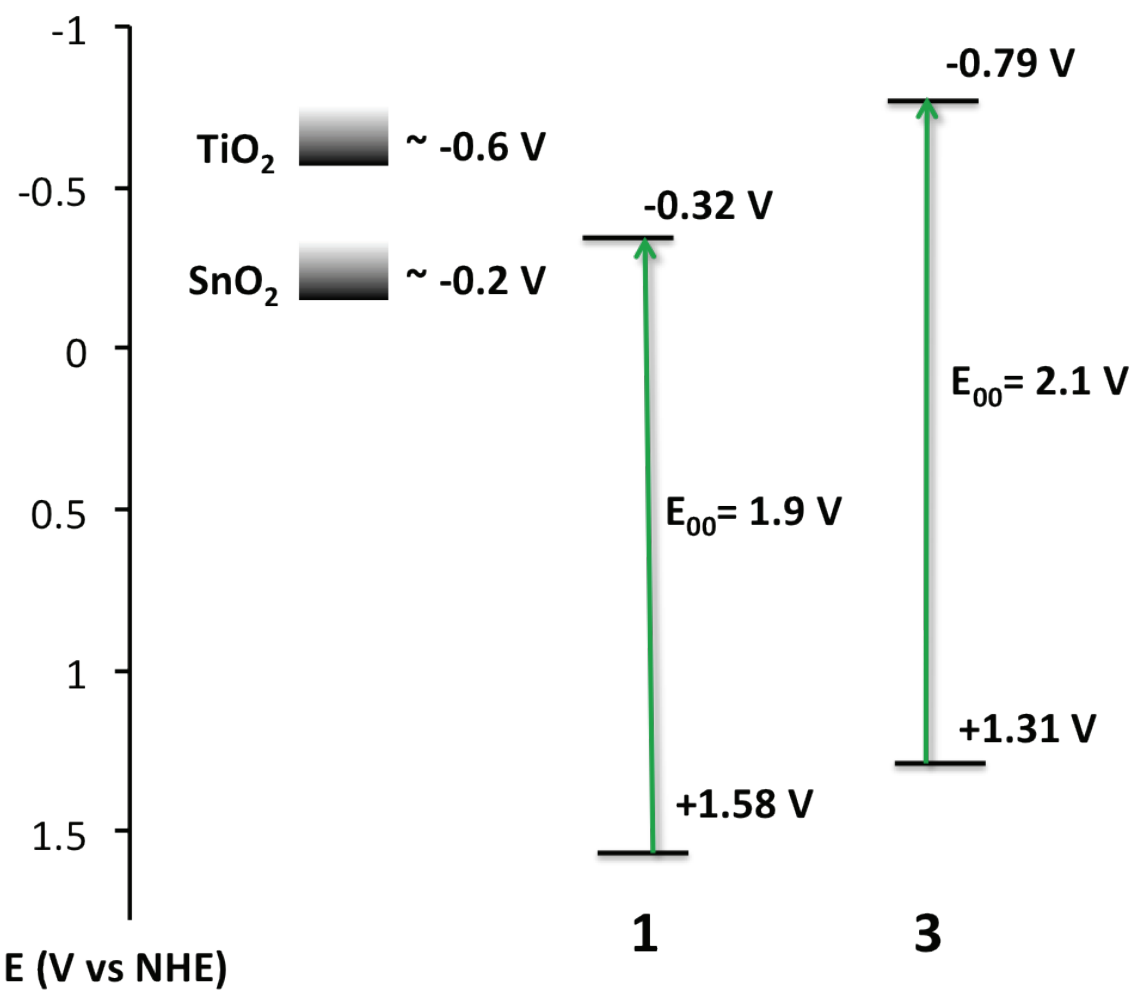


Figure S13: Ground and excited-state energy levels of **1** and **3** with comparison to the conduction bands of TiO_2 and SnO_2 at pH 7.⁸

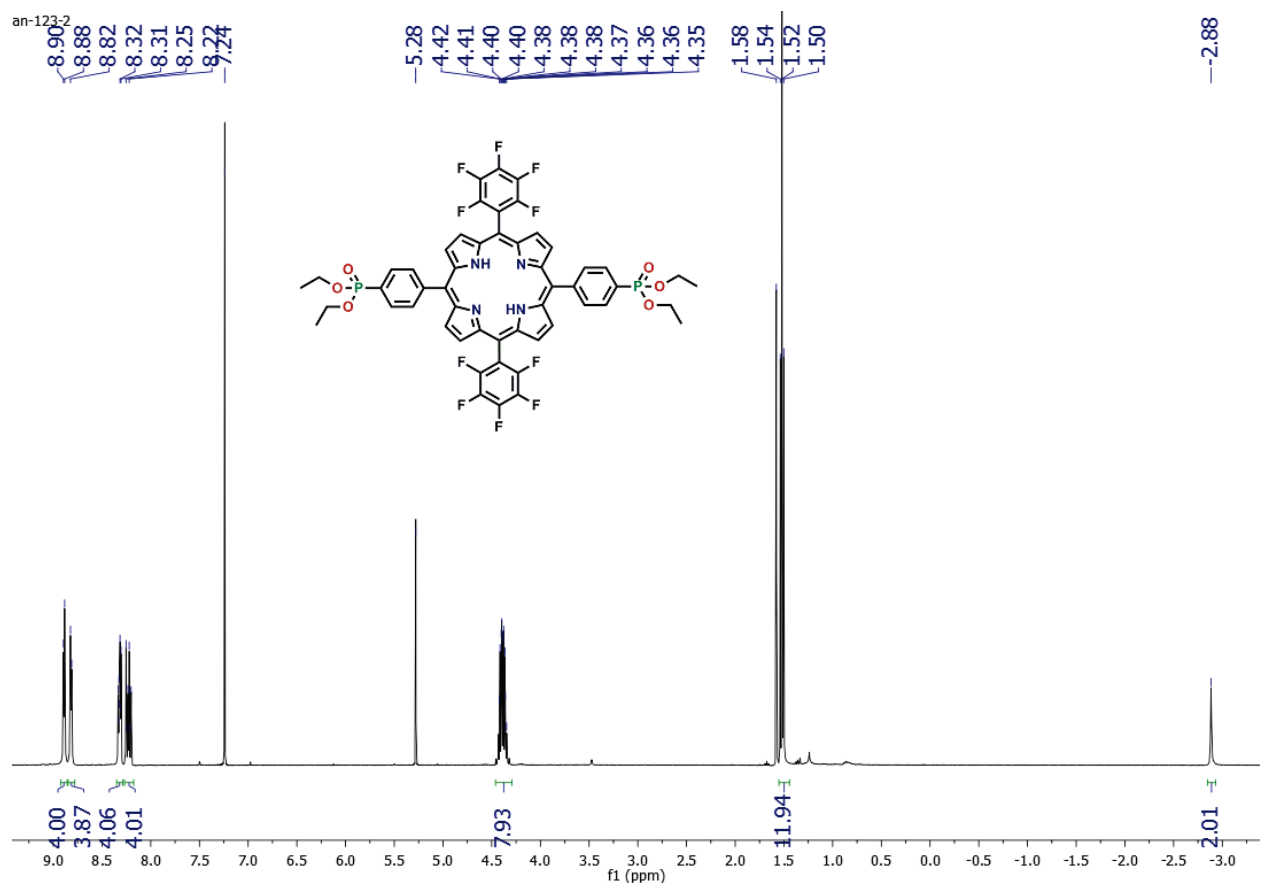


Figure S14: ^1H NMR of phosphonated porphyrin **5** in CDCl_3

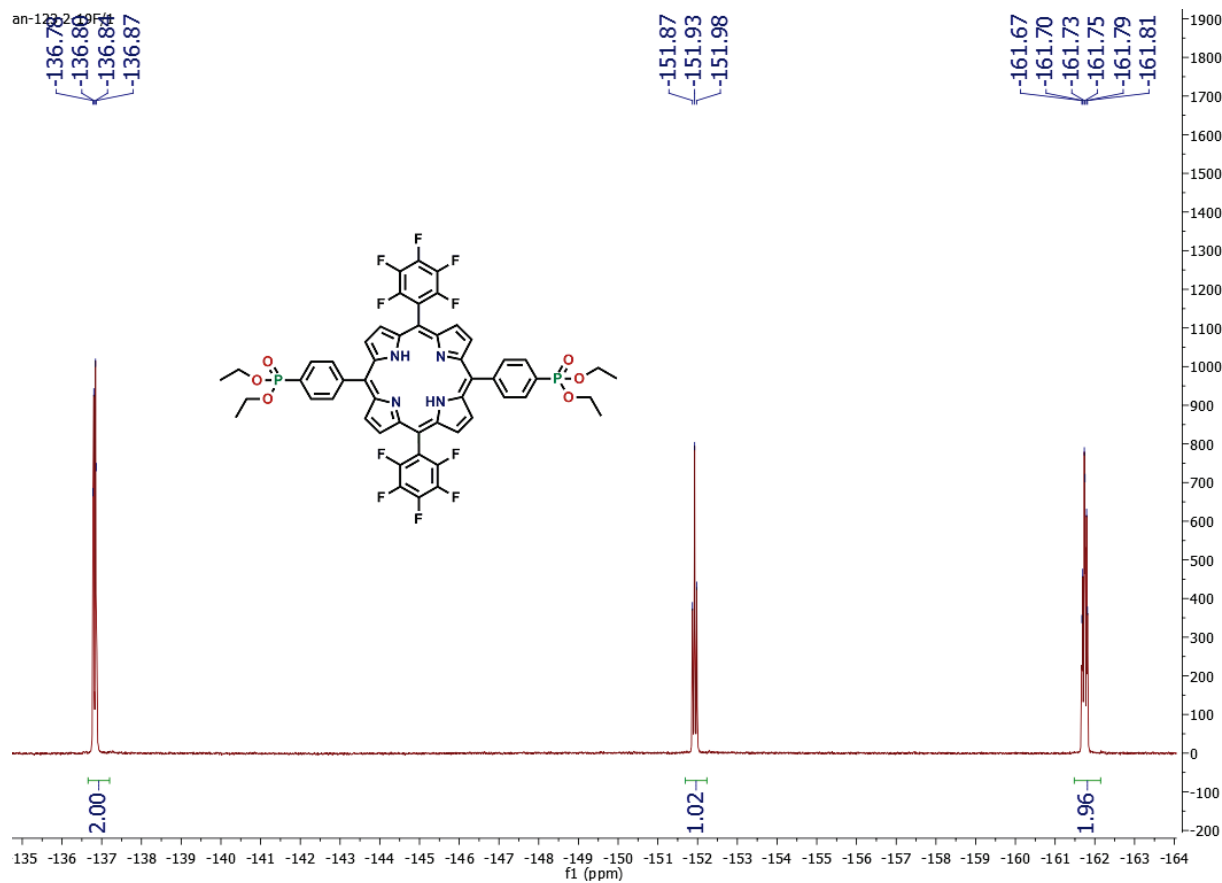


Figure S15: ^{19}F NMR of phosphonated porphyrin **5** in CDCl_3

-18.60

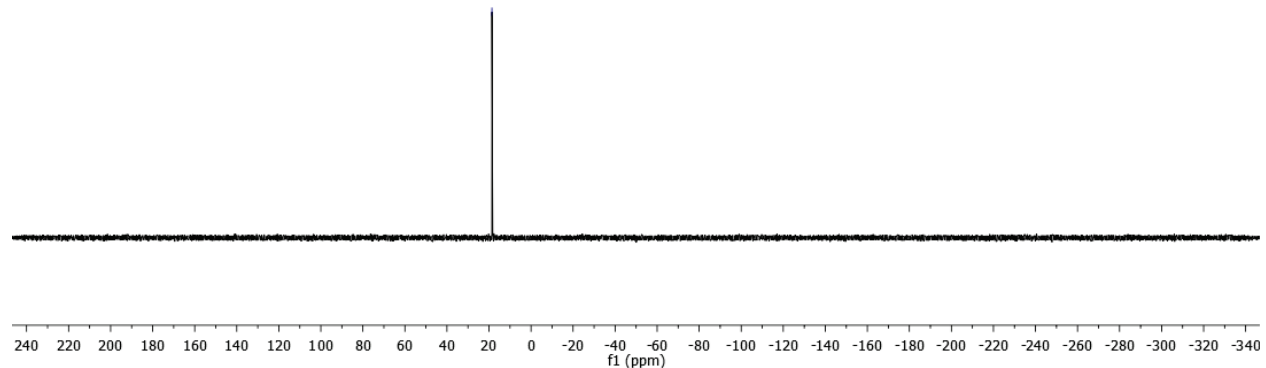
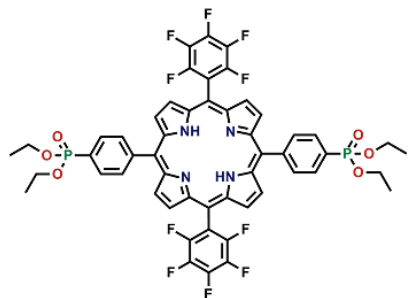


Figure S16: ^{31}P NMR of phosphonated porphyrin **5** in CDCl_3

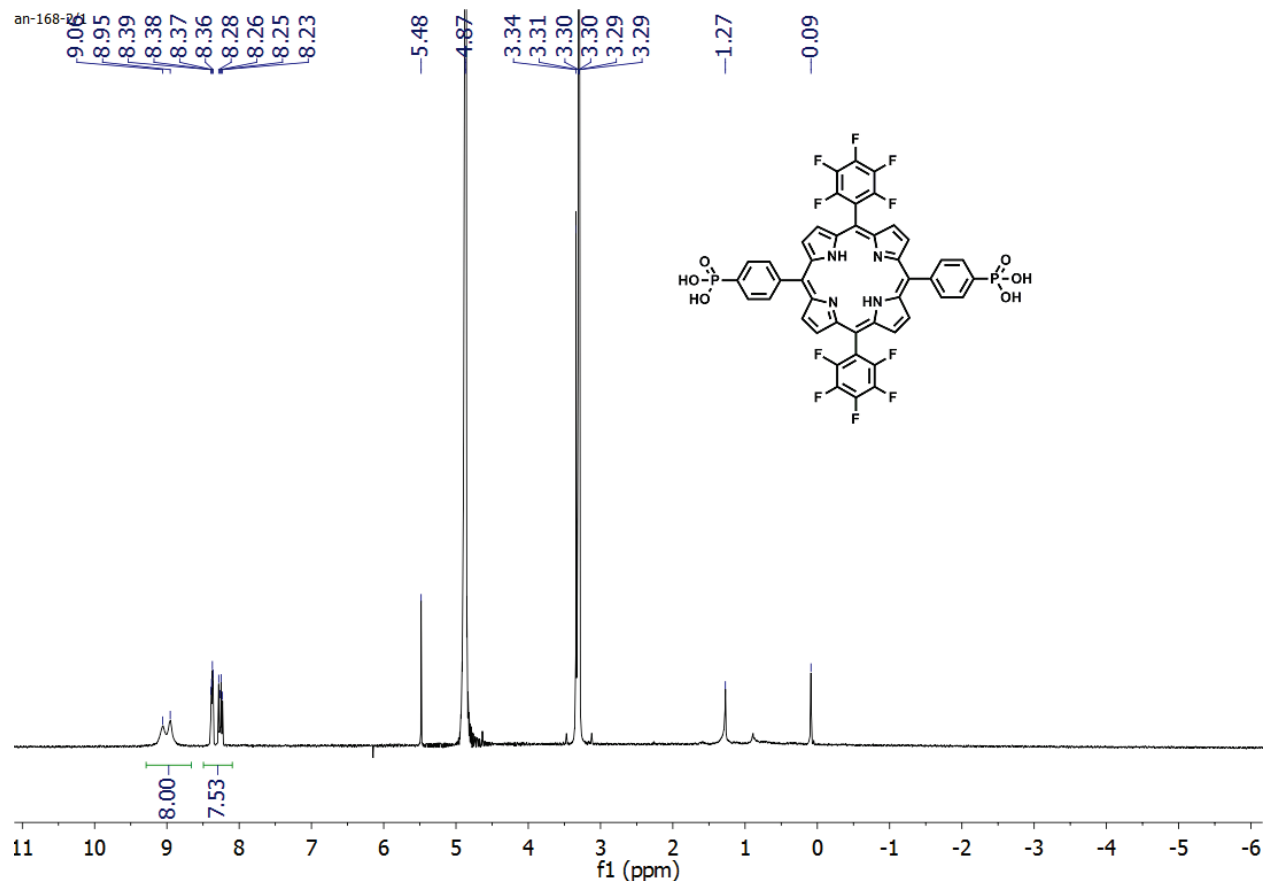


Figure S17: ^1H NMR of **1** in CD_3OD

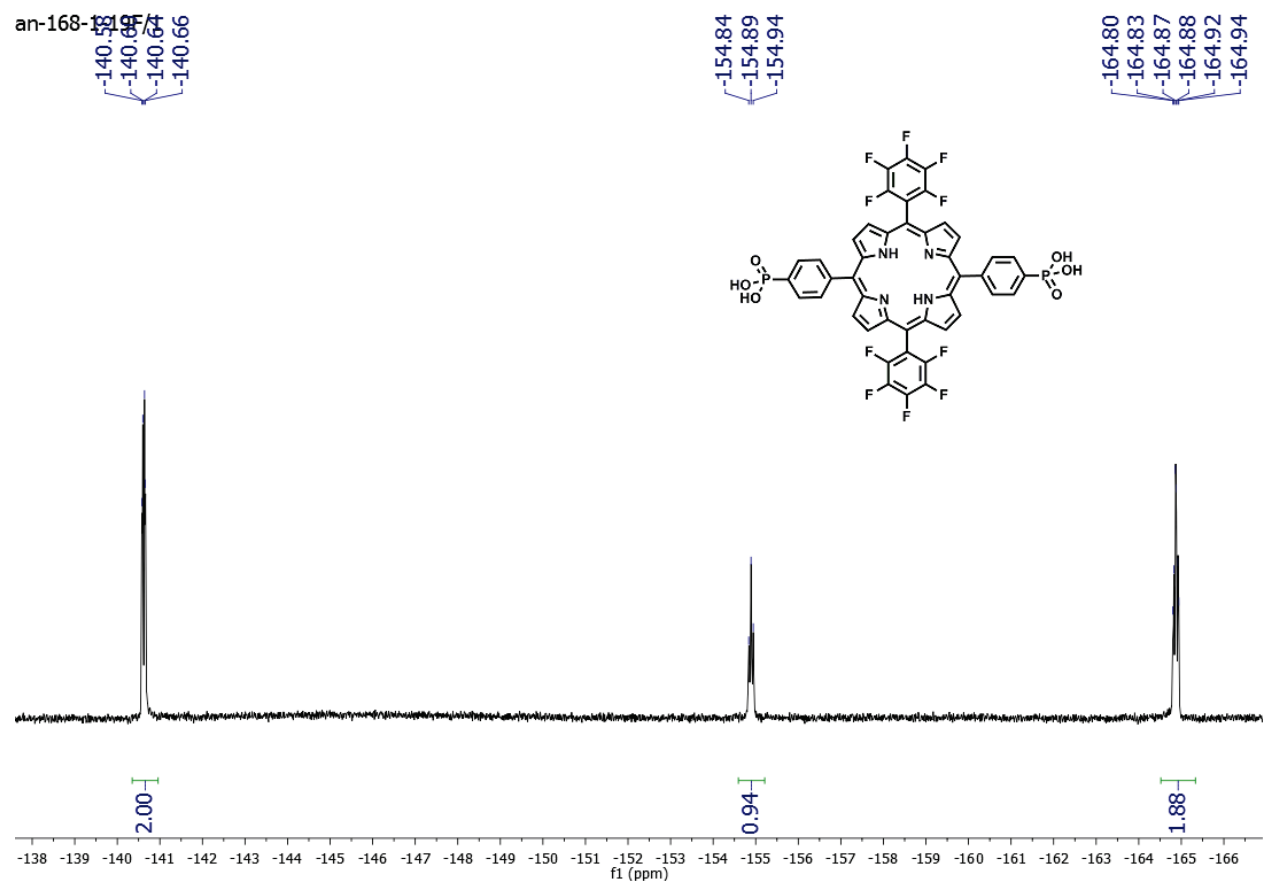


Figure S18: ^{19}F NMR of **1** in CD_3OD

-15.47

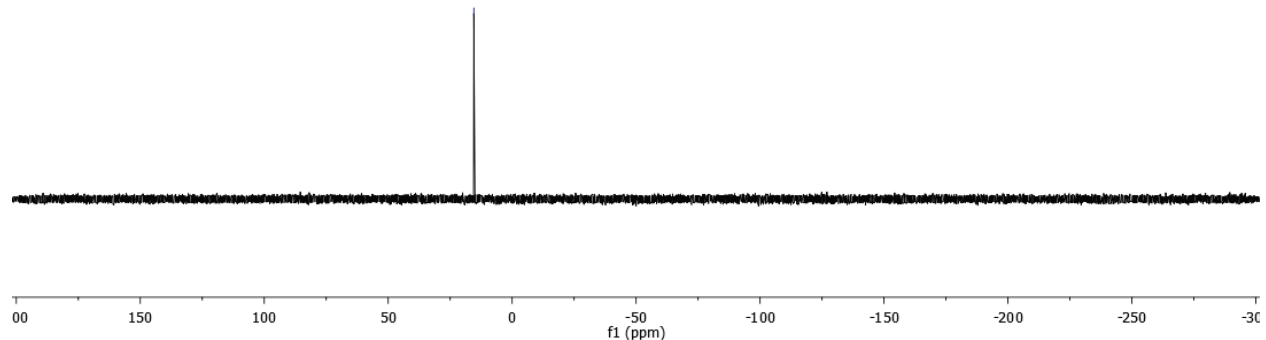
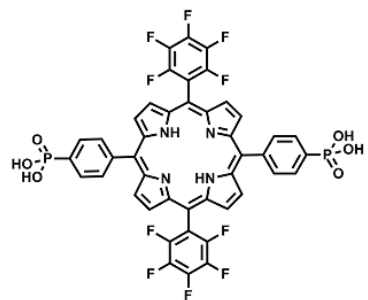


Figure S19: ^{31}P NMR of **1** in CD_3OD

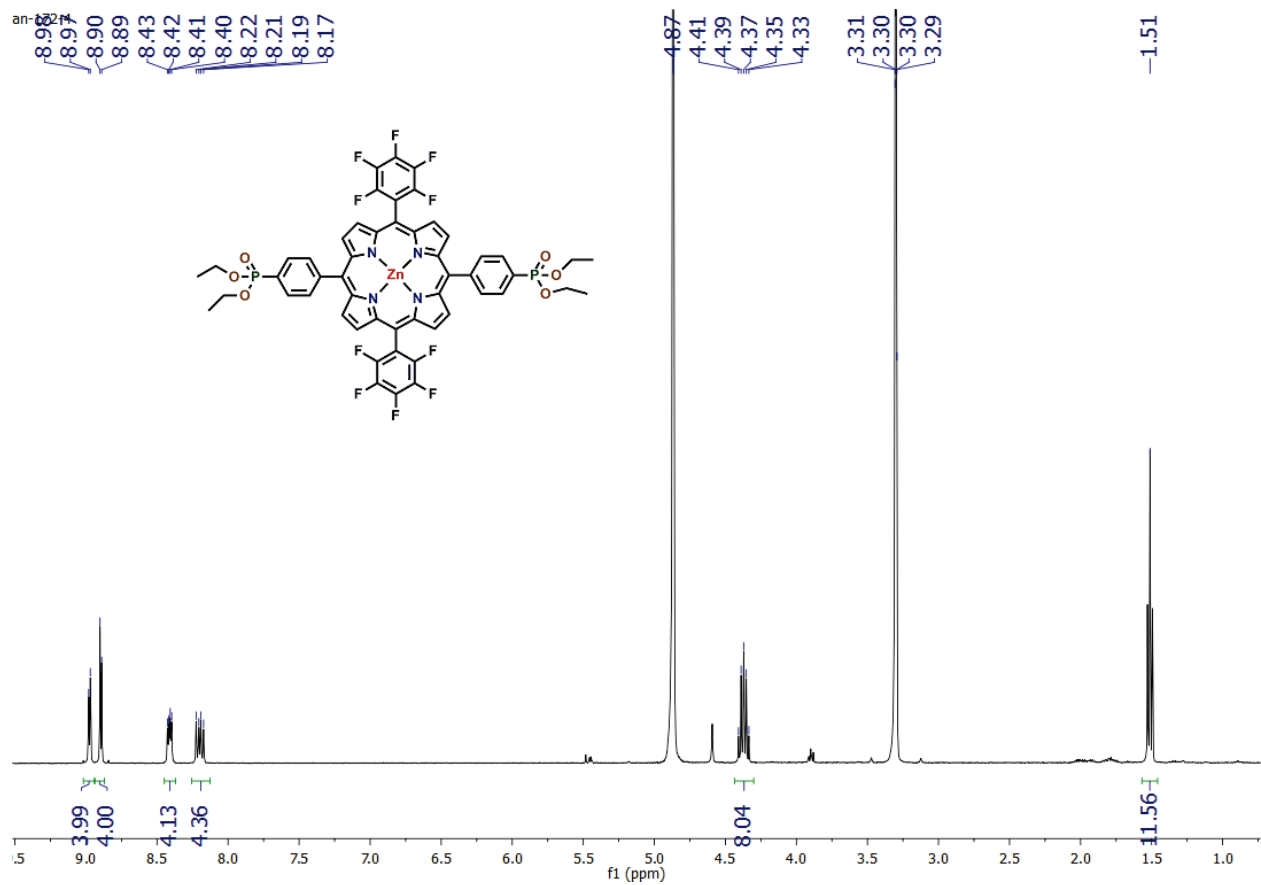


Figure S20: ^1H NMR of **6** in CD_3OD

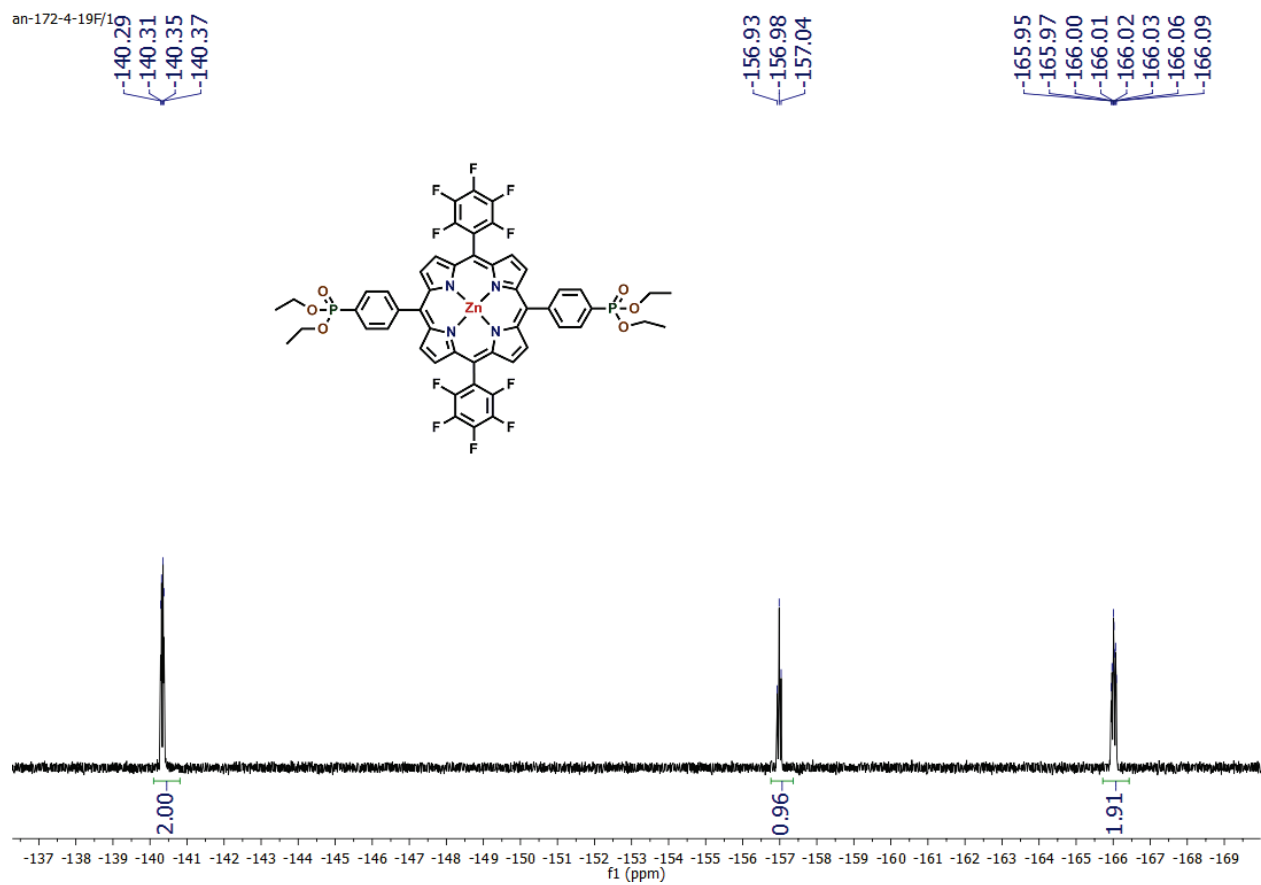


Figure S21: ^{19}F NMR of **6** in CD_3OD

1955
1943

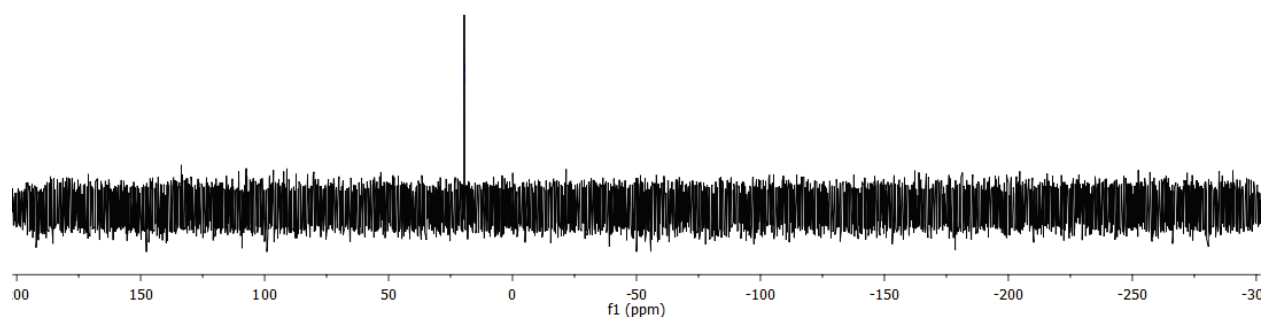
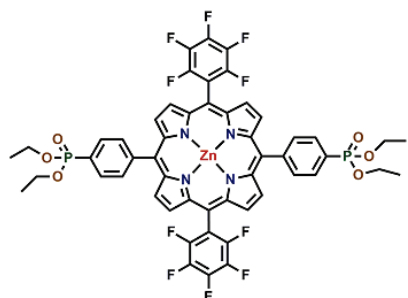


Figure S22: ³¹P NMR of **6** in CD₃OD

XPS Full TiO₂_Zr:2(14018_TiO2-Zr_PoZr_Ru)
Acqn. Time(s): 241 Spectrum Lens Mode:Hybrid Resolution:Pass energy 80
Sweeps: 1 Anode:Mono(Al(Mono))150 W Step(meV): 1000.0
Dwell Time(ms): 200 Charge Neutraliser :On Acquired On :14/02/11 14:16:55

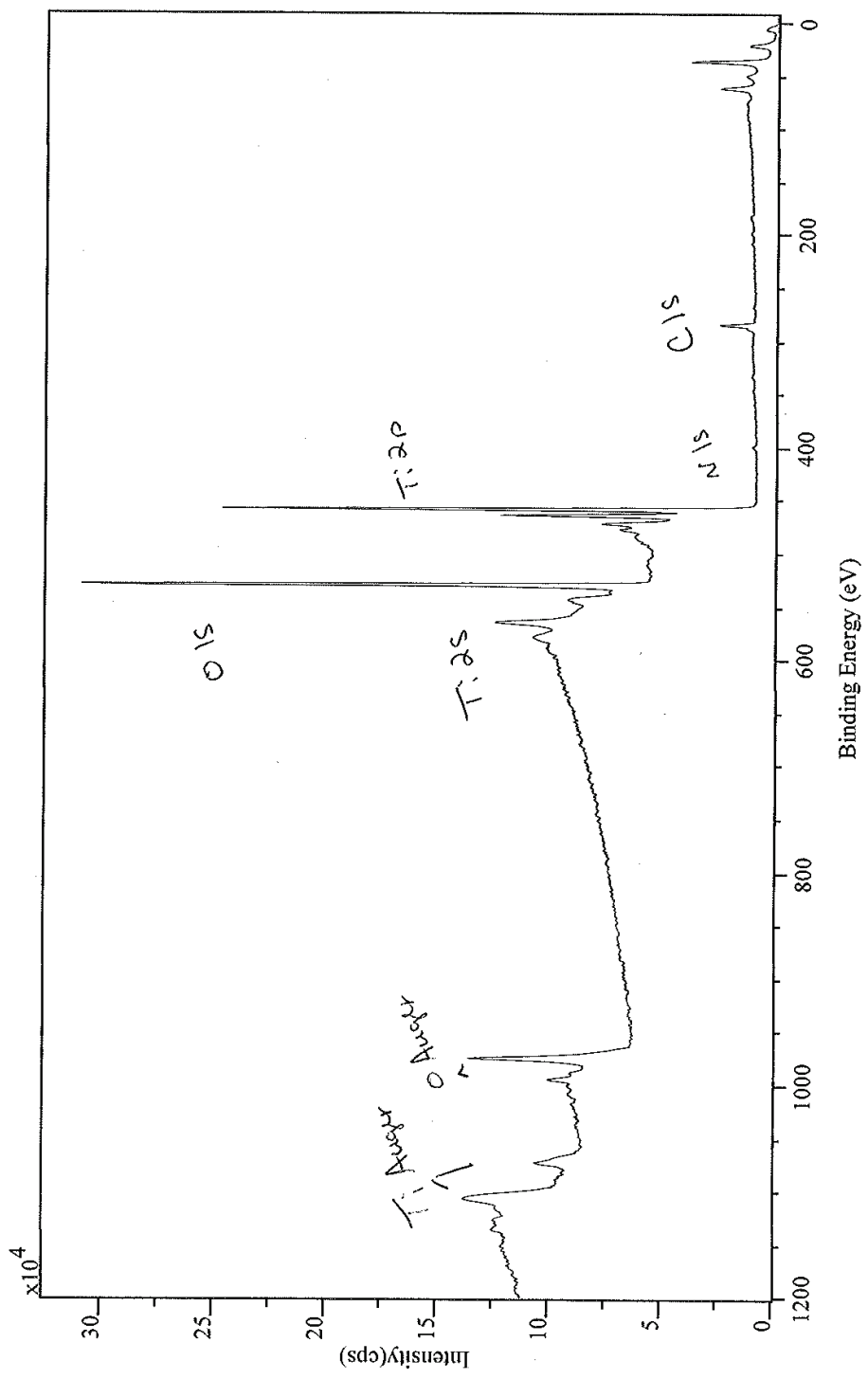


Figure S23: XPS of TiO₂-1-Zr-2

Table S1: X-ray photoelectron spectroscopy (XPS) of TiO₂–**1**–Zr–**2**

	N/Ru ratio	P/Ru ratio	F/Ru ratio
TiO ₂ – 1 –Zr– 2	11.7	4.1	13.8 ¹
Ideal	11	4	10

¹Deviations from ideal may be due to fluorine contributions from PF₆ anion and FTO.

References

- (1) Knauf, R. R.; Brennaman, M. K.; Alibabaei, L.; Norris, M. R.; Dempsey, J. L. *J. Phys. Chem. C* **2013**, *117*, 25259.
- (2) Lee, S.-H. A.; Abrams, N. M.; Hoertz, P. G.; Barber, G. D.; Halaoui, L. I.; Mallouk, T. E. *J. Phys. Chem. B* **2008**, *112*, 14415.
- (3) Song, W.; Glasson, C. R. K.; Luo, H.; Hanson, K.; Brennaman, M. K.; Concepcion, J. J.; Meyer, T. J. *Journal of Physical Chemistry Letters* **2011**, *2*, 1808.
- (4) Pavlishchuk, V. V.; Addison, A. W. *Inorganica Chimica Acta* **2000**, *298*, 97.
- (5) Laha, J. K.; Dhanalekshmi, S.; Taniguchi, M.; Ambroise, A.; Lindsey, J. S. *Org. Proc. Res. Dev.* **2003**, *7*, 799.
- (6) Muthukumaran, K.; Loewe, R. S.; Ambroise, A.; Tamaru, S. I.; Li, Q. L.; Mathur, G.; Bocian, D. F.; Misra, V.; Lindsey, J. S. *J. Org. Chem.* **2004**, *69*, 1444.
- (7) Concepcion, J. J.; Jurss, J. W.; Norris, M. R.; Chen, Z.; Templeton, J. L.; Meyer, T. J. *Inorg. Chem.* **2010**, *49*, 1277.
- (8) Kavan, L.; Tétreault, N.; Moehl, T.; Grätzel, M. *J. Phys. Chem. C* **2014**, ASAP. DOI: 10.1021/jp4103614